

Solvothermal Synthesis, Characterization and Optical Properties of ZnO and ZnO-Al₂O₃ Mixed Oxide Nanoparticles.

Ehsan Zamani, Fatemeh Rezaei, Sara Bagheri, Mahdieh Ghobadifard, Maryam Mahmoudi, Saeid Farhadi, Abedin Zebardasti and Alireza Aslani*

Department of Chemistry, Faculty of Sciences, Lorsetan University, Lorestan-Khoramabad, Iran.

Received: 20 Jul. 2014, Revised: 18 Oct. 2014, Accepted: 27 Oct. 2014.

Published online: 1 Jan. 2015.

Abstract: ZnO-Al₂O₃ mixed oxide nanoparticles were successfully produced from a solution containing Zn (acetate) and AlCl₃ by Solvothermal method. The calcination process of the ZnO-Al₂O₃ composite nanoparticles brought forth polycrystalline two-phase ZnO-Al₂O₃ nanoparticles of 30–50 nm in diameters. ZnO and Al₂O₃ were crystallized into würtzite and rock salt structures, respectively. The optical properties of ZnO-Al₂O₃ nanoparticles were determined with solid state UV and florescent (PL). The structure properties of this sample were analyzed by XRD, SEM and Raman spectroscopy and then comparison with baulk case of these samples.

Keywords: Nanoparticles, Solvothermal; X-ray diffraction; mixed oxide.

1. Introduction

Solvothermal reactions are widely used for the synthesis of solids such as porous, magnetic or electronic compounds as well as catalysts and pigments. The discovery or optimization of new compounds is closely connected with the exploration of the parameter space, which normally comprises of compositional and process parameters. These can range from molar ratios of the starting materials or their order of addition, the pH of the starting mixture and the solvent employed in the synthesis to the reaction time and temperature. While investigations studying one parameter at a time are straightforward, the simultaneous study of many reaction variables dramatically raises the number of necessary reactions. The serial investigation of such large parameter spaces is impractical and most often infeasible, and high-throughput methods are a more appropriate way.

In recent years, controllable synthesis and ordered assembly of nano-crystalline materials is one of the most interesting research areas due to their potential applications in optical and electronic fields, biological labeling and catalysis [1–3]. Their unique properties depend on both the size and the morphology of the nano-crystalline materials. A variety of methods have been developed to synthesise

nano-crystalline materials with different morphologies. Among them, the traditional method of fabrication of chalcogenide semiconductor is solid synthesis at high temperature (≥ 500 °C), i.e., VLS (vapor–liquid–solid growth), CVT (chemical vapor transport growth) and thermolysis of single source. Nowadays, more attentions have been paid to solid synthesis at low temperature, such as electrochemistry, supersonic method, hydrothermal and solvothermal process [4–6]. Hydro-solvothermal method is direct, fast and easily than other methods for synthesis of nanomaterials [7–9].

On the other hand the metal oxides are extremely important technological materials for use in electronic and photonic devices. In these metal oxides, zinc oxide (ZnO) is very appropriate for insulation applications due to their low heat capacity and high melting point [10]. Another application for Al₂O₃ and ZnO are as fundamental materials for chemical heat pump [11], as substrate materials for the epitaxial growth of thin films with desirable magnetic and electronic properties [12]. During the past several years, various methods have been developed for the synthesis of nanomaterials that have included template-assisted [13], vapor liquid solid (VLS) [14], colloidal micelle [15] and electrochemical processes [16]. Because the novel properties of nanomaterials depend on their size and shape,

*Corresponding author e-mail: a.aslani110@yahoo.com

new synthetic strategies and a better understanding of the growth mechanisms by which the size and shape of nanostructures can be easily tailored are key issues in nanomaterials science. The synthesis and fabrication of nanoscale controlled materials are rapidly developing fields of materials science [17].

Particularly, hollow nanostructures have attracted much attention because their unique shape makes them applicable as delivery vehicles, fillers as well as for catalysis, and could bring about changes in physical and chemical properties [18,19]. Several chemical techniques, such as co-precipitation, sol-gel and hydrothermal methods, etc, have been used to prepare nanocrystalline powders [20]. Among these chemical techniques, the hydrothermal process has attracted a great deal of attention since particles with the desired characteristics can be prepared with this technique by controlling the solution pH, reaction temperature, reaction time, solute concentration and the types of solvent depending on the particular application [21]. The main advantages of hydrothermal synthesis are related to homogeneous nucleation processes, ascribed to elimination of the calcinations step to produce very low grain sizes and high purity powders [22]. Zinc oxide (ZnO) is a wide band-gap semiconductor with unique physical properties and a wide range of potential applications. It has already been used for applications such as sensors, transparent coating for solar cells and acoustic devices. ZnO has also recently attracted considerable interest for efficient ultraviolet LEDs and laser devices. Indeed, it is an excellent candidate for high-temperature and high-efficiency optoelectronic applications owing to its large excitation binding energy (60 meV), the largest among conventional semiconductors [23-28].

2. Experimental Section

2.1 Synthesis of ZnO-Al₂O₃ nano particles.

A solution of Zn (AC)₂ (2 mmol) and AlCl₃ (2 mmol) in EtOH/H₂O solvent (30 mL) was added to a solution of NaOH (6 mmol) in EtOH/H₂O solvent (10 mL) at room temperature under stirring. After 30 min stirring the mixture transferred into Teflon-lined stainless steel autoclaves, sealed, and maintained at 150 °C for 24 h. Subsequently, the reactor was cooled down to room temperature immediately. The resulting white solid products were centrifuged, washed with distilled water and ethanol to remove the ions possibly remaining in the final products, and finally dried at 60 °C in air. The obtained samples were characterized by X-ray powder diffraction.

2.2 Synthesis of ZnO nano particles.

A solution of Zn(AC)₂ (2 mmol) in EtOH/H₂O solvent (20 mL) was added to a solution of NaOH (4 mmol) in EtOH/H₂O solvent (10 mL) at room temperature under stirring. After 30 min stirring the mixture transferred into

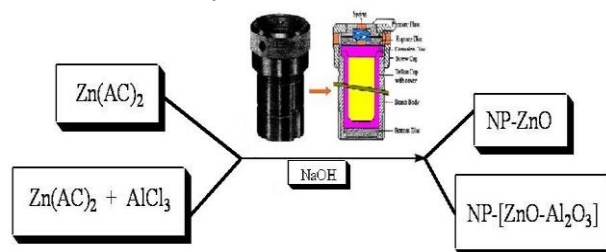
Teflon-lined stainless steel autoclaves, sealed, and maintained at 150 °C for 24 h. Subsequently, the reactor was cooled down to room temperature immediately.

The resulting white solid products were centrifuged, washed with distilled water and ethanol to remove the ions possibly remaining in the final products, and finally dried at 60 °C in air. The obtained samples were characterized by X-ray powder diffraction.

The resulting with solid products were centrifuged, washed with distilled water and ethanol to remove the ions possibly remaining in the final products, and finally dried at 60 °C in air. The obtained samples were characterized by X-ray powder diffraction, solid state UV, solid state florescent and Raman spectroscopy. The wave amplitude in each experiment was adjusted as needed. X-ray powder diffraction (XRD) measurements were performed using a Philips diffractometer of X'pert Company with mono chromatized CuK_α radiation. The samples were characterized with a scanning electron microscope (SEM) (Philips XL 30) with gold coating. Raman spectra were recorded on a Labram HR 800-Jobin Yvon Horbiba spectrometer.

3. Result and discussion

3.1 Structural study



Scheme 1 Shows the reaction between Zn (AC)₂, AlCl₃ and sodium hydroxide to formation ZnO and ZnO-Al₂O₃ nanoparticles.

The reaction between Zn(AC)₂ and AlCl₃ and sodium hydroxide to form ZnO and ZnO-Al₂O₃ nanoparticles has been shown in scheme 1.

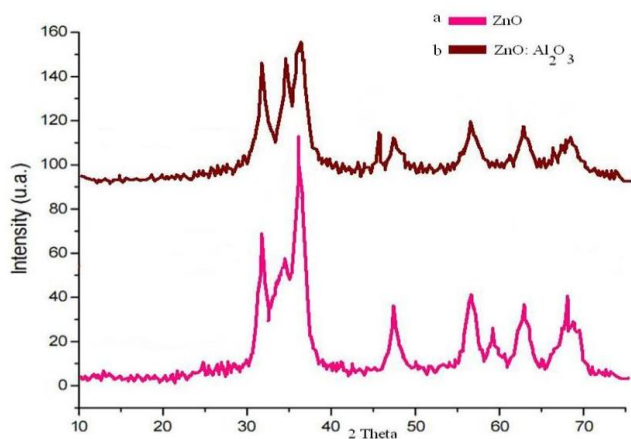


Fig.1 X-Ray powder diffraction pattern of (a) ZnO nanoparticles and (b) ZnO-Al₂O₃ nanoparticles.

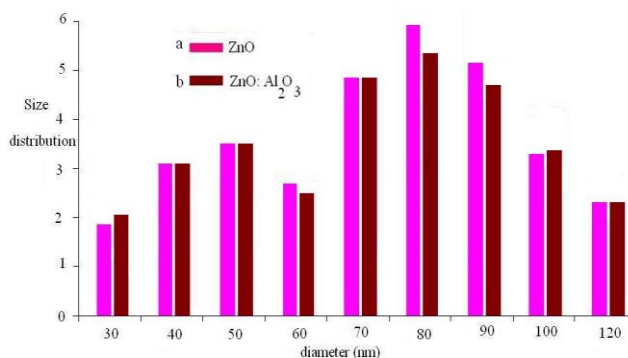
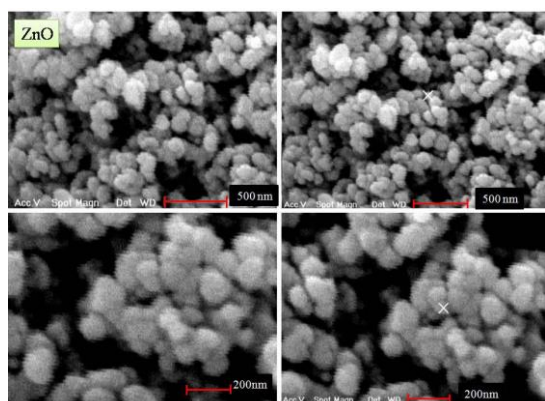
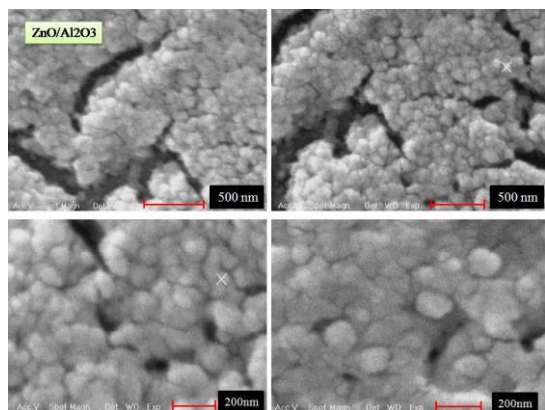


Fig.3 Particle size histogram of the (a) ZnO and (b) ZnO-Al₂O₃ nanoparticles.

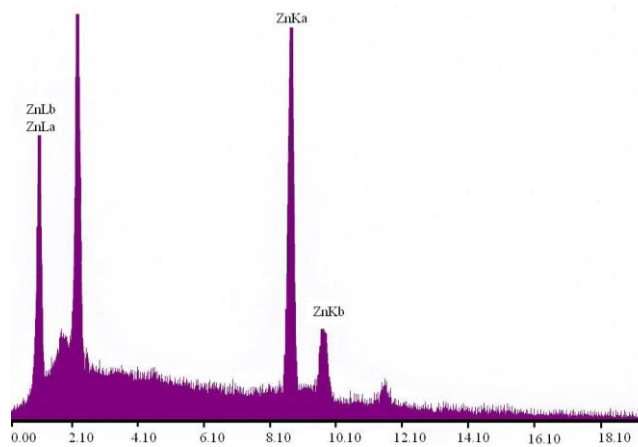


(a)

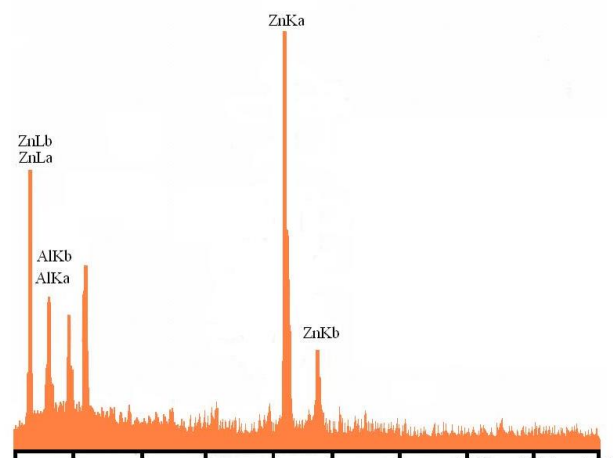


(b)

Fig.2 The SEM images of the (a) ZnO and (b) ZnO-Al₂O₃ nanoparticles.



(a)



(b)

Fig.4 EDAX analysis of the (a) ZnO and (b) ZnO-Al₂O₃ nanoparticles.

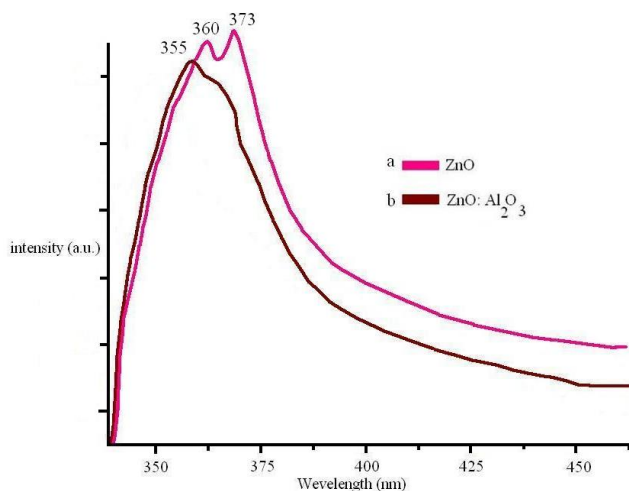


Fig.5 Solid state absorption spectrum of (a) ZnO and (b) ZnO-Al₂O₃ nanoparticles ($\lambda_{\text{exc}}=320$).

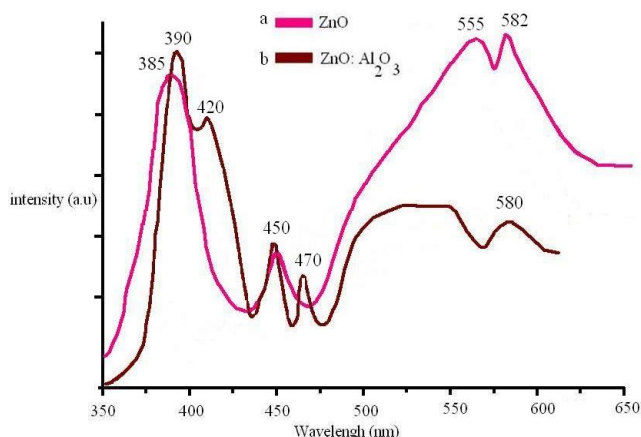


Fig.6 Solid state PL spectra of the (a) ZnO and (b) ZnO-Al₂O₃ nanoparticles ($\lambda_{\text{exc}}=320$).

In the XRD spectra of ZnO and ZnO-Al₂O₃ nanoparticles we can observe the formation of well crystalline hexagonal structure. On the other hand XRD spectra show that there was no other phase corresponding to Al₂O₃. Sharp diffraction peaks shown in Fig. 1(a and b) indicate good crystalline of ZnO and ZnO-Al₂O₃ nanoparticles. No characteristic peak related to any impurity was observed. The broadening of the peaks indicated that the particles were of nanometer scale.

The morphology, structure and size of the samples are investigated by Scanning Electron Microscopy (SEM). Fig.2 (a and b) indicates that the original morphology of the ZnO and ZnO-Al₂O₃ nanoparticles are approximately spherical with the diameter varying between 30 to 60 nm. To investigate the size distribution of the nanoparticles, a particle size histogram was prepared for ZnO and ZnO-Al₂O₃ nanoparticles in Fig. 3(a and b). Most of the particles possess sizes in the range from 30 to 60 nm. For further

demonstration, the EDAX was performed for the ZnO and ZnO-Al₂O₃ nanoparticles.

The EDAX spectrum given in Fig.4 (a and b) shows the presence of Zn and Zn-Al as the only elementary components in the ZnO and ZnO-Al₂O₃ nano particles respectively.

Fig. 5(a and b) shows the solid state UV-vis adsorption spectra of ZnO and ZnO-Al₂O₃ nano particles. Compare to ZnO-Al₂O₃, maximum adsorption wave-lengths of ZnO have 4-6 nm red shift. As shown in Fig.5 (a and b), the UV-vis adsorption spectrum indicated the maximum adsorption wave-lengths of ZnO and ZnO-Al₂O₃ nanoparticles were 355, 360 and 373 nm, respectively. ZnO nanoparticles have 4-6 nm red-shifts.

In Figure 6, the representative PL spectra of the samples are presented. In general, the room temperature PL spectra of all the as-grown and annealed samples revealed similar features. There appeared four emission band at about 385, 450, 555 and 582 nm and for ZnO-Al₂O₃ five emission band at about 390, 420, 450, 470 and 580 nm generally assigned as a near-band-edge (NBE) emission band. The position of the NBE emission band in our nanostructures agrees well with the reported value for the nanoparticles grown by thermal evaporation. Generally, the deep-level emission in ZnO and ZnO-Al₂O₃ consists of green emissions around 555 nm and near-yellow emissions around 580 nm. Though the origin of the green emission is controversial, generally it is assigned to the singly ionized oxygen vacancies. The yellow emissions have been related to the interstitial O_i in ZnO and ZnO-Al₂O₃. Therefore, the evolution of green and yellow bands in ZnO and ZnO-Al₂O₃ are competitive with each other. The broad emission band revealed in the visible region in our samples is due to the superposition of green and yellow emissions. On air annealing, the intensity ratio of deep-level emission and NBE emission ($I_{\text{deep-level}}/I_{\text{NBE}}$) decreased from 6.8 to about 0.44 due to annealing out of point defect and defect complexes.

4. Conclusion

We could develop a simple low-temperature hydro-solvothermal method to synthesize single crystalline, hexagonal ZnO and ZnO-Al₂O₃ nanostructures with different ratio. By controlling the initial and final pH of the reaction mixture, ZnO and ZnO-Al₂O₃ nanostructures of different ratio could be grown through controlling the nucleation and growth rates. The 1D nanostructures grow preferentially along the [002] c axis with low strain.

The crystal quality of the nanostructures could further be improved through reduction of strain and deep-level defects by annealing them in air. Though several low-temperature chemical or hydro-solvothermalsynthesis of ZnO and ZnO-Al₂O₃ nanoparticles have been reported. Our low-temperature synthesis method allows to synthesize

ZnO nanostructures of several morphologies in a controlled manner. However ZnO and ZnO-Al₂O₃ nanopowders prepared by solvothermal method without any stabilizer or additive. The ZnO and ZnO-Al₂O₃ particle size was controlled by varying the temperature and aging time of the reaction in solvothermal reactor. The ZnO particle size distributions determined from SEM images and PL spectra data for the ZnO and ZnO-Al₂O₃ solid state were in good agreement. The PL results for the ZnO and ZnO-Al₂O₃ nanoparticles showed significant defects in their morphology due to their large surfaces, while the green emission peak in the nano particles was due to a decrease in the amount of excitations. Additionally, the optical results showed a blue-shift of the UV peak for the sample that was placed in the low temperature zone, which occurred due to the effect of Al on the band-gap of the ZnO nanostructures.

Acknowledgements

Supporting of this investigation by Lorestan University (Khorramabad, Islamic Republic of Iran) and KimyaJavid Company, Gitipasand industrial company, (Isfahan. Islamic Republic of Iran) is gratefully acknowledged.

REFERENCES

- [1] H.F. Chen, B.H. Clarkson, K. Sun, J.F. Mansfield, *J. Colloid Interface Sci.* **288**, 97, (2005).
- [2] Y. Liu, J. Zhan, M. Ren, K. Tang, W. Yu, Y. Qian, *J. Mater. Res. Bull.* **36**, 1231, (2001).
- [3] Y. Hu, J.F. Chen, W.M. Chen, *J. Adv. Funct. Mater.* **14**, 383, (2004).
- [4] A.N. Banerjee, K.K. Chattopadhyay, *J. Appl. Phys.* **97**,084308, (2005).
- [5] C.B.Murray,D.J.Norris, M.G. Bawendi, *J. Am.Chem. Soc.* **115**,8706, (1993).
- [6] H. Travis, M. Larsen, Sigman, A. Ghezelbash, R.C. Doty, B.A. Korgel, *J. Am. Chem. Soc.* **125**, 5638, (2003).
- [7] A. Aslani, A. Morsali, V. T. Yilmaz, C. Kazak, *J. Molecular Structure*, **929**, 187, (2009).
- [8] A. Aslani, A. Morsali, *Inorganica Chimica Acta*, **362**, 5012, (2009).
- [9] A. Aslani, A. Morsali, M. Zeller, *Solid State Sciences*, **10**, 1591, (2008).
- [10] M.C. Wu, J.S. Corneille, C.A. Estrada, J.W. He, D.W. Goodman, *Chem. Phys. Lett.* **182**, 472, (1991).
- [11] Y. Kato, F. Takahashi, A. Watanabe, Y. Yoshizawa, *Appl. Therm. Eng.* **21**, 1067, (2001).
- [12] K.L. Klug, V.P. Dravid, *Appl. Phys. Lett.* **21**, 1687, (2002).
- [13] Y.J. Han, J. Kim, G.D. Stucky, *Chem. Mater.* **12**, 2068, (2000).
- [14] J. Hu, T.W. Odom, C.M. Lieber, *Acc. Chem. Res.* **32**, 435, (1999).
- [15] C.C. Chen, C.Y. Chao, Z.H. Lang, *Chem. Mater.* **12**, 1516, (2000).
- [16] M.B. Mohamed, K.Z. Ismail, S. Link, M.A. El-Sayer, *J. Phys. Chem.* **102**, 9370, (1998).
- [17] Xia Y, *Halas NJ. MRS Bull.* **30**, 356, (2005).
- [18] Kim SW, Kim M, Lee WY, Hyeon T. *J Am ChemSoc.* **124**, 7642, (2002).
- [19] Sun Y, Xia Y. *J. Am. ChemSoc.* **126**, 3892, (2004).
- [20] Kim, B. C., Kim, S. M., Lee, J. H. and Kim, J. J.. *J. Am. Ceram. Soc.* **85**(8), 2083–2088, (2002).
- [21] Lee, J. S. and Choi, S. *C. Mater. Lett.* **58**, 390–393, (2004).
- [22] Piticescu, R. R., Monty, C., Taloi, D., Motoc, A. and Axinte, S. *J. Eur. Ceram. Soc.* **21**, 2057–2060, (2001).
- [23] M.G. Kim, U. Dahmen, AlanW. Searcy, *J. Am. Ceram. Soc.* **71** (8), 373–375, (1988).
- [24] C. Feldmann, S. Matschulo, S.Ahlert, *J. Mater. Sci.* **42** (17), 7076–7080, (2007).
- [25] I. Halibia, P. Neou-Syngouna, D. Kolitsa, *Thermochim. Acta*, **320**, 75, (1998).
- [26] G. Duan, X. Yang, J. Chen, G. Huang, L. Lu, X. Wang, *Powder Technol.* **172** (1), 27–29, (2007).
- [27] P. Pisciella, S. Crisucci, A. Karamanov, M. Pelino, *Waste Manage.* **21** (1), 1–9, (2001).
- [28] R.T. Rajeswara, *Chem. Eng. Technol.* **19**, 373, (1996).